Proc. Of the 8th International E-Conference on Advances in Engineering, Technology and Management - ICETM 2022

ISBN: 978-1-63248-195-5 DOI: 10.15224/ 978-1-63248-195-5-13

Empirical Relationship To Explicate Mudflow Behaviour

Budijanto Widjaja and Livia Florencia

***Abstract*— Mudflow is one of the natural disasters that frequently happen in Indonesia. This flow-type of landslide occurs suddenly and moves very fast, so it can cause massive damage and loss. However, knowledge about this disaster's behavior is minimal, even though it poses a huge destructive threat. Assessment from twenty case studies is done to understand more about mudflow behavior. High plasticity silt is the soil type most likely to become mudflow. The sediment concentration by volume value for mudflow is in the range of 0.29–0.56. Eight relationships between mudflow parameters were obtained: the steeper the slope, the greater the flow distance; as the liquidity index increases, the viscosity and yield stress value will decrease; the higher the viscosity, the greater the flow width; More volume moves from sources to deposition areas over longer flow distances; as flow rate increases, flow duration decreases; the deeper the flow depth, the shorter the flow duration. Lastly, a wider flow width means the flow distance will also increase.**

Keywords*— *duration, flow depth, landslide, mudflow, viscosity, yield stress

I. Introduction

Mudflow is categorized as fast-moving landslides [1], so this natural disaster must be considered dangerous because it has a massive potential destructive force. Mudflow mainly consists of fine-grained soils. The rise of its water content can trigger the flow. Mudflow is a type of mass movement with a flow characteristic different from other landslide types, so Mohr-Coulomb Theory cannot explain the behavior. A rheological approach, such as Bingham Model, is used to find out more about mudflow behavior. This model has parameters, namely viscosity and yield stress.

In this study, rheology parameters along with soil parameters (e.g., soil type, Atterberg limits, water content) and flow parameters (e.g., flow distance, flow width, flow depth) from past mudflow case studies in Indonesia, Taiwan, Korea, China, Chile, and Italy are collected. This study also aims to propose an empirical relationship to explain the mudflow behavior based on those data.

II. Literature Review

Mudflow is a flow-type landslide composed of soil-water mixtures and sometimes other materials that move at high speed. The flow velocity can reach 0.05 m/s (very rapid) and up to more than 5.0 m/s (extremely rapid) [2].

Budijanto Widjaja and Livia Florencia
Department of Civil Engineering, Parahyangan Catholic University
Indonesia

The rheological approach, which is the study of material flow, is used to comprehend mudflow behavior. Mudflow is defined as saturated soils moving downhill under gravitational attraction. These rapid movements can generate huge impulsive loads on objects that the flow bumps into [3]. Mudflow is initiated when the water content reaches or exceeds the soil's liquid limit ($w \geq LL$). That means mudflow happens when the soil is in a viscous liquid state. Flowing materials can be grouped into Newtonian or non-Newtonian fluids, in which mudflow is considered a non-Newtonian fluid.

Bingham Model, as seen in Fig. 2, is a rheology model to describe non-Newtonian fluid with parameters (i.e., Viscosity, Yield stress). Viscosity (η) is a value that depicts the inner force of fluids to resist the flow movement. Yield stress (τ_y) is the minimum stress value needed to make the material flow. In other words, when material stress is lower than the yield stress, the materials are in a plastic state. However, when material stress is higher than yield stress, the flow-movement of the material will occur.

Proc. Of the 8th International E-Conference on Advances in Engineering, Technology and Management - ICETM 2022

ISBN: 978-1-63248-195-5 DOI: 10.15224/ 978-1-63248-195-5-13

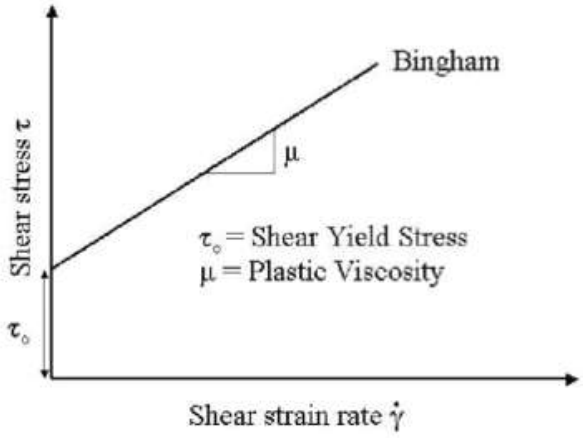

Figure 1. Bingham Model [4]

Generally, a mudflow is divided into three areas: source area, transportation area, and deposition area, as shown in Fig. 2. Source area is the area where flow is initiated with high velocity because shear stress on soil material is larger than the yield stress (τ_y). In the transportation area, referred to as the main track, mudflow will follow along the shape of natural channels on the slope. The flow velocity in this area will decrease because viscosity will slow down the flow. Once the flow gets into the deposition area, the flow will stop because soil stress has already reduced and is lower than the yield stress (τ_y).

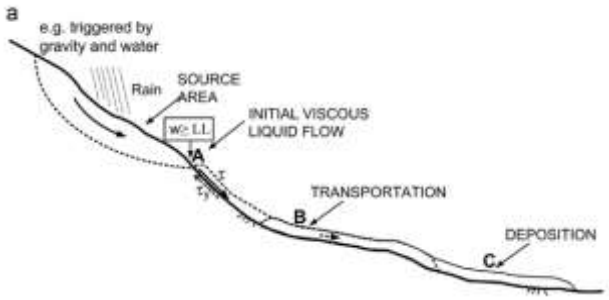

Figure 2. Side-view of the Mudflow Areas [5]

III. Methods and Data

A. *Mudflow Characteristic*

Three criteria can be applied to determine whether the mass movement counted as a mudflow which are:

- Solid concentration by volume (C_v)

  Solid concentration by volume is a parameter that describes the ratio of the soil's dry weight and the total volume of the soil-water mixture. The value is defined as

$$C_v = \frac{1}{1 + w * G_s} \quad (1)$$

  where w is water content, and G_s is the specific gravity of soils. A C_v value of 0.45-0.55 indicates that the mass movement is a mudflow [6].

- Liquidity Index

  The liquidity index is a value to portray the soil phase. This parameter can be defined as

$$LI = \frac{w - PL}{LL - PL} \quad (2)$$

ISBN: 978-1-63248-195-5 DOI: 10.15224/ 978-1-63248-195-5-13

where w is water content, PL is the plastic limit, and LL is the liquid limit of the soil. Mudflow occurs in a viscous liquid state, which means the liquidity index value is equal to or greater than 1.

- Width-length ratio

  Based on the top view of the mudflow, the average width (B) and flow distance (L) from the source area to a deposition can be measured. Mass movement with a width-length ratio of 0.05-0.3 is considered a mudflow [7].

B. Data Collection

Twenty mudflow case studies from Indonesia, Taiwan, Korea, China, Chile, and Italy are assessed. Soil parameters, flow parameters, and rheology parameters are collected from case studies recorded as secondary data for this paper. Soil parameters include the soil type based on the Casagrande plasticity chart, specific gravity, water content (w), liquid limit (LL), plasticity limit (PL), plasticity index (PI), liquidity index (LI), and solid concentration by volume (C_v) value as presented in Table 2. Rheology parameters consist of viscosity (η) and yield stress (τy), as seen in Table 1.

TABLE I. RHEOLOGY PARAMETERS

No.	Location	τ_y	η	*Sources*
		[kPa]	[Pa.s]	
1	Pakuon,Sukaresmi	1.41	0.014	[9]
2	Pramen, Bantar	2.33	0.100	[10]
3	Karangrejo, Purworejo	3.50	0.170	[11]
4	Mogol, Karanganyar	3.00	0.120	[12]
5	Tenjolaya, Bandung	1.40	0.010	[12]
6	Margamukti, Pangalengan	1.83	0.078	[13]
7	Banaran, Ponorogo	4.33	0.010	[14]
8	Pasir Panjang, Brebes	2.45	0.513	[15]
9	Songan, Bangli	3.67	0.020	[16]
10	Sirnaresmi, Sukabumi	3.36	0.800	[17]
11	Mukapayung, Cililin	1.38	0.040	[18]
12	Jemblung, Banjarnegara	1.46	0.200	[19]
13	Honje, Parungponteng	3.68	0.200	[20];[21]
14	Margoyoso, Magelang	5.00	0.050	[22]; [23]
15	Sukajaya, Bogor	2.63	1.316	[24]
16	Maokong, Taiwan	2.10	0.050	[12]
17	Umyeonsan, South Korea	0.99	0.193	[25]; [26]
18	Villa Santa Lucia, Chile	1.75	0.629	[27]
19	Dagou, China	5.00	0.587	[28]; [29]; [30]
20	Dolomites, Italy	4.60	0.060	[31]

Flow parameters, as presented in Table 3, consist of slope angle, flow dimension (i.e., flow width, flow distance, flow depth), flow duration, flow rate, volume that moved from the source area to the deposition area, and flow velocity. Flow width and distance can be measured from the top view of mudflow as illustrated in Fig. 3. Flow duration, flow rate, volume, and flow velocity obtained from simulation.

ISBN: 978-1-63248-195-5 DOI: 10.15224/ 978-1-63248-195-5-13

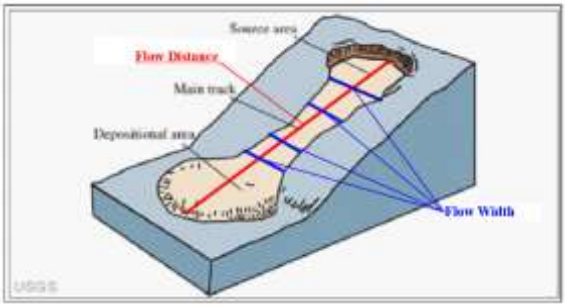

Figure 3. Flow width and distance measurement illustration (modified from USGS, 2004)

TABLE II.

SOIL PARAMETERS

No.	*Location*	*Soil Type*	G_s	*w* *[%]*	*LL*	*PL*	*PI*	*LI*	C_v	**Sources**
1	Pakuon,Sukaresmi	MH	2.55	87.12	66.00	47.52	18.48	2.14	0.31	[9]
2	Pramen, Bantar	ML	2.48	82.50	75.75	41.75	34.00	1.20	0.33	[10]
3	Karangrejo, Purworejo	MH	2.56	73.62	73.62	37.95	35.67	1.00	0.35	[11]
4	Mogol, Karanganyar	MH	2.71	53.00	53.00	34.00	19.00	1.00	0.41	[12]
5	Tenjolaya, Bandung	ML	2.63	53.19	45.00	32.00	13.00	1.63	0.42	[12]
6	Margamukti, Pangalengan	MH	2.78	75.00	75.00	43.00	32.00	1.00	0.32	[13]
7	Banaran, Ponorogo	MH	2.74	60.00	60.00	45.00	15.00	1.00	0.38	[14]
8	Pasir Panjang, Brebes	MH	2.65	92.00	91.55	52.52	39.03	1.01	0.29	[15]
9	Songan, Bangli	SC	2.68	37.00	36.10	18.62	17.48	1.05	0.50	[16]
10	Sirnaresmi, Sukabumi	MH	2.89	63.27	66.10	51.80	14.30	0.80	0.35	[17]
11	Mukapayung, Cililin	MH	2.74	64.36	58.00	29.93	28.07	1.23	0.36	[18]
12	Jemblung, Banjarnegara	MH	2.74	72.99	64.83	40.32	24.51	1.33	0.33	[19]
13	Honje, Parungponteng	MH	2.52	69.64	68.55	36.64	31.91	1.03	0.36	[20];[21]
14	Margoyoso, Magelang	SM	2.65	65.00	63.64	41.58	22.06	1.06	0.37	[22]; [23]
15	Sukajaya, Bogor	MH	2.72	55.14	63.05	37.98	25.07	0.68	0.40	[24]
16	Maokong, Taiwan	ML	2.66	33.00	33.00	26.00	7.00	1.00	0.53	[12]
17	Umyeonsan, South Korea	CL	2.70	32.10	31.60	22.30	9.30	1.05	0.54	[25]; [26]
18	Villa Santa Lucia, Chile	CH	2.65	56.60	50.00	27.00	23.00	1.29	0.40	[27]
19	Dagou, China	ML	2.73	39.00	38.02	24.25	13.77	1.07	0.48	[28]; [29]; [30]
20	Dolomites, Italy	ML	2.75	28.00	20.00	4.00	16.00	1.50	0.56	[31]

Proc. Of the 8th International E-Conference on Advances in Engineering, Technology and Management - ICETM 2022

ISBN: 978-1-63248-195-5 DOI: 10.15224/ 978-1-63248-195-5-13

Based on the rheology parameters collected in Table 1, it can be seen that 18 out of 20 case studies have a viscosity value of less than 1. A lower viscosity value indicates that the resisting forces within the material are also reduced, allowing the soil mass to flow more easily. Yield stress values from 20 case studies vary between 0.99 kPa and 5 kPa. With a higher yield stress value, the stress when mudflow is initiated will also increase.

From soil parameters collected in Table 2, it can be determined that high plasticity silt is the soil type that is most likely to become mudflow. Besides that, it also can be seen from the table that 90 percent of mudflow cases happen when the water content is equal to, or more than the liquid limit and the liquidity index has a value of 1 or higher. This conclusion verifies the theory that mudflow occurs in a viscous liquid state. In addition, the obtained C_v values from Table 2 are in the range of 0.29-0.56. These ranges are larger than the range given by [6].

In Table 3, it can be seen that the width-length ratio is in the range of 0.02 – 0.53. These ranges are more significant than the range recommended by [7]. Five case studies fall outside the recommended value. In this table, it can be concluded that mudflow in Chile is the biggest mudflow disaster compared to 19 other case studies. This conclusion is reached because Chile mudflow has a steep slope with the longest flow distance, widest flow width, biggest flow rate and volume, and highest velocity than all other case studies. The documentation from this disaster shown in Fig. 4

Figure 4. Villa Santa Lucia, Chile Mudflow Documentation [8]

TABLE III. FLOW PARAMETERS

No.	*Location*	*Slope Angle, θ*	*Flow Distance, L*	*Flow Width, B*	*Width-length ratio*	*Flow Depth, h*	*Flow Duration, t*	*Flow Rate, Q*	*Volume, V*	*Flow Velocity, u*	**Sources**
		[°]	*[m]*	*[m]*		*[m]*	*[menit]*	*[m3/s]*	*[m3]*	*[m/s]*	
1	Pakuon,Sukaresmi	30.00	268.00	20.00	0.07	2.40	20.00	0.50	600.00	2.80	[9]
2	Pramen, Bantar	35.00	650.00	89.00	0.14	0.90	38.00	3.77	4751.66	1.10	[10]
3	Karangrejo, Purworejo	30.00	225.00	83.00	0.37	1.95	12.40	4.00	7127.49	3.80	[11]
4	Mogol, Karanganyar	21.00	275.00	45.00	0.16	1.00	18.00	5.00	5400.00	2.80	[12]
5	Tenjolaya, Bandung	61.00	800.00	40.00	0.05	2.40	12.62	50.00	31280.00	7.80	[12]
6	Margamukti, Pangalengan	60.00	620.00	183.00	0.30	8.70	15.00	55.00	49500.00	9.47	[13]
7	Banaran, Ponorogo	40.00	1010.00	112.00	0.11	11.30	15.00	144.44	120000.00	16.70	[14]
8	Pasir Panjang, Brebes	45.00	2300.00	140.00	0.06	8.60	15.00	393.94	354545.00	10.90	[15]
9	Songan, Bangli	45.00	748.37	41.34	0.06	4.30	12.00	712.50	213750.00	4.20	[16]
10	Sirnaresmi, Sukabumi	28.00	645.00	129.00	0.20	4.00	2.35	2424.06	78539.82	19.80	[17]
11	Mukapayung, Cililin	40.00	1000.00	20.00	0.02	0.20	54.00	1.11	2000.00	1.30	[18]

ISBN: 978-1-63248-195-5 DOI: 10.15224/ 978-1-63248-195-5-13

No.	*Location*	*Slope Angle, θ*	*Flow Distance, L*	*Flow Width, B*	*Width-length ratio*	*Flow Depth, h*	*Flow Duration, t*	*Flow Rate, Q*	*Volume, V*	*Flow Velocity, u*	**Sources**
		[°]	*[m]*	*[m]*		*[m]*	*[menit]*	*[m3/s]*	*[m3]*	*[m/s]*	
12	Jemblung, Banjarnegara	35.00	500.00	80.00	0.16	4.60	15.00	186.98	56092.52	4.40	[19]
13	Honje, Parungponteng	30.00	120.00	64.00	0.53	1.65	12.00	15.72	4716.00	7.10	[20];[21]
14	Margoyoso, Magelang	22.15	130.00	30.00	0.23	3.50	4.00	1069.91	805.87	18.01	[22]; [23]
15	Sukajaya, Bogor	45.00	450.00	77.80	0.17	5.30	5.00	63.08	19015.55	8.00	[24]
16	Maokong, Taiwan	29.00	275.00	15.00	0.05	8.60	3.60	40.83	36751.53	6.00	[12]
17	Umyeonsan, South Korea	37.00	650.00	35.00	0.05	8.00	2.00	650.00	6500.00	10.30	[25]; [26]
18	Villa Santa Lucia, Chile	79.00	8600.00	506.67	0.06	5.00	5.00	16666.67	5000000.00	20.00	[27]
19	Dagou, China	29.20	1380.00	44.10	0.03	3.50	20.00	730.00	190000.00	7.20	[28]; [29]; [30]
20	Dolomites, Italy	35.00	1632.00	50.00	0.03	2.50	11.00	71.00	6000.00	9.00	[31]

IV. Results and Discussion

Fig. 5 shows the relationship between the slope angle and the measured flow distance. The obtained trendline indicates that these parameters have a positive correlation, which means a steeper slope will produce a longer flow distance. On the contrary, a gentler slope will reduce the flow distance from the source area to the deposition area. This trendline can be represented by a power equation, as seen in Eq. (3).

$$L = 0.0019\ \theta^{3.5} \quad (3)$$

Longer flow distance means this mudflow disaster will affect a bigger area. Therefore, modification of slope geometry can be done to reduce the damage due to mudflow disasters. But this remedial measure must be done along with a proper drainage system.

The relationship between liquidity index and viscosity (η) can be seen in Fig. 6. The trend shows that these parameters have a negative correlation. So as the liquidity index gets bigger, the viscosity value will decrease. On the other hand, a smaller liquidity index means a higher viscosity value. Eq. (4) stands for the trendline between liquidity index and viscosity.

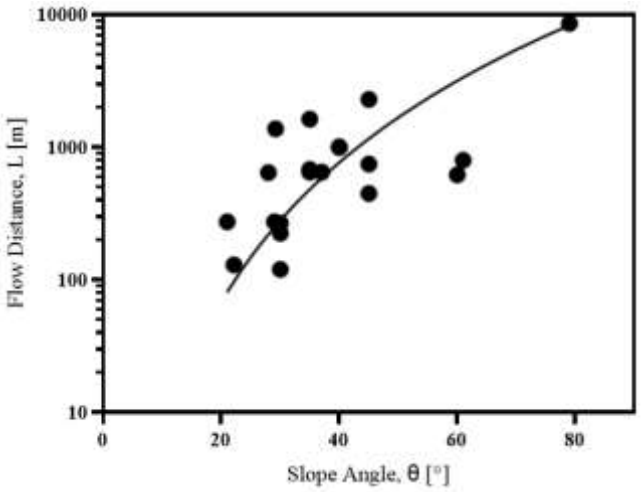

Figure 5. Slope Angle-Flow Distance Relationship

$$\eta = \frac{0.1872}{LI^{5.142}} + 0.005 \quad (4)$$

This relationship is linked to the water content. That is because a larger liquidity index means the water content is increasing and exceeding the liquid limit.

ISBN: 978-1-63248-195-5 DOI: 10.15224/ 978-1-63248-195-5-13

But as water content increases, the viscosity value will decrease. Hence, the correlation between these parameters is negative.

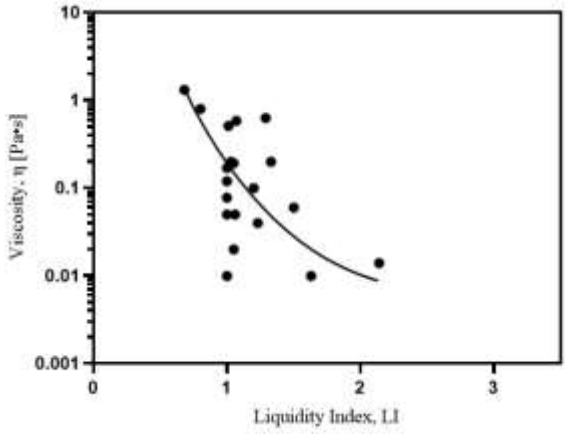

Figure 6. Liquidity Index-Viscosity Relationship

Fig. 7 displays the relationship between the liquidity index and yield stress. The trendline shows that these parameters have a negative correlation. So as the liquidity index increases, the yield stress will decrease. On the other side, yield stress will be higher if the liquidity index is smaller. The equation that represents this relationship can be seen in Eq. (5).

$$\tau_y = \frac{1.885}{LI^{5.815}} + 1.153 \quad (5)$$

Similar to the liquidity index-viscosity relationship, this relationship is also associated with the water content. A larger liquidity index means the water content is rising. But soil shear strength will reduce when the water content increase; consequently, the yield stress will also decrease. Thus, the liquidity index and yield stress have a negative correlation.

Fig. 8 depicts the relationship between viscosity and flow width. The trendline shows a positive correlation. As the viscosity value increases, the flow width will also be larger. Conversely, the flow width will be smaller with a lower viscosity value. This relationship can be represented by a power equation, as seen in Eq. (6).

$$B = 150.2\ \eta^{0.741} + 24.58 \quad (6)$$

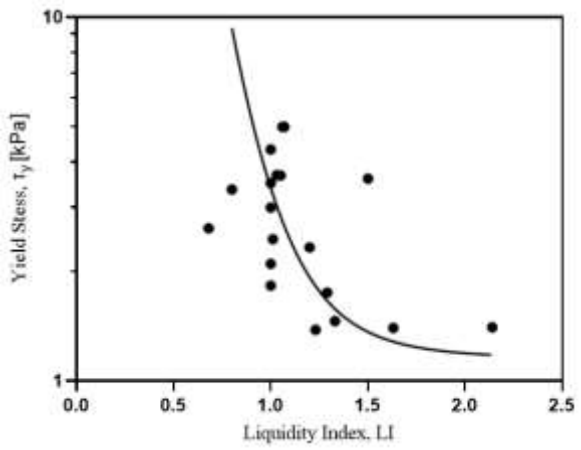

Figure 7. Liquidity Index-Yield Stress Relationship

From the viscosity-flow width relationship, it can be concluded that mudflow with a larger viscosity will have a widened flow shape. On the contrary, narrowed flow shape means the mudflow has a low viscosity.

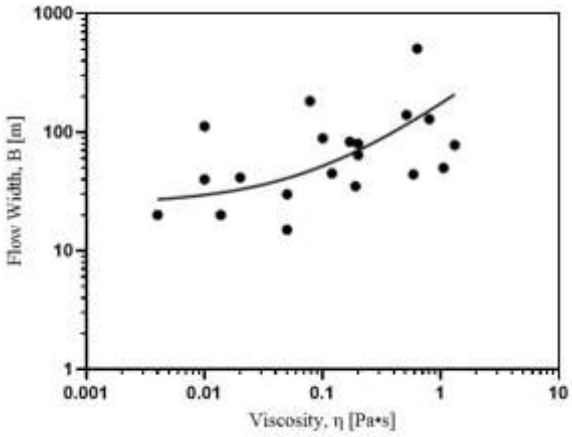

Figure 8. Viscosity-Flow Width Relationship

The relationship between flow distance and the volume that moves from the source area to the deposition area can be seen in Fig. 9. The trendline shows that these parameters have a positive correlation, which means that as flow distance increases, the volume will also be larger. On the other hand, as the flow distance decreases, the volume is smaller. The equation representing this volume can be seen in Eq. (7).

$$V = 0.4613\ L^{1.756} - 2386 \quad (7)$$

The volume calculated by Eq. (7) is the volume in the source area, which is assumed to be the same as in the deposition area. That means this relationship is achieved under the assumption that no material is added to the transportation area. In the actual mudflow disaster, there will be at least erosion or other materials carried away in the transportation area. This assumption is made because it is challenging to calculate the additional volume from the transportation area.

ISBN: 978-1-63248-195-5 DOI: 10.15224/ 978-1-63248-195-5-13

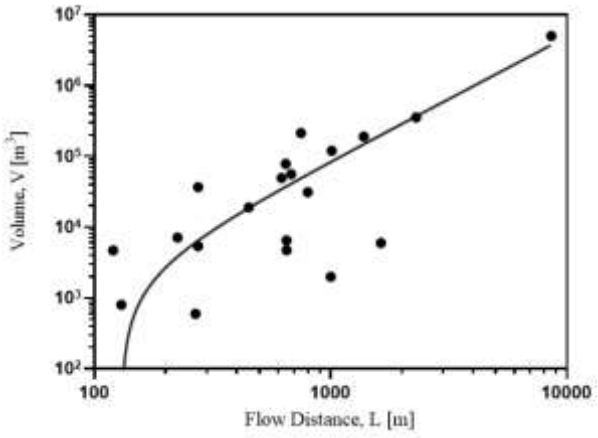

Figure 9. Viscosity-Flow Width Relationship

Fig. 10 shows the relationship between flow rate and flow duration. The trendline obtained has a negative correlation. So as the flow rate increases, the flow duration will decrease. On the contrary when the flow rate decrease, the flow duration will increase. Eq. (8) is the equation that represents this relationship.

$$t = \frac{105}{Q^{0.03}} - 78 \tag{8}$$

A larger flow rate will make the mudflow more dangerous. It is because a higher flow rate means a larger volume is moved in a short time from the source area to the deposition area. Besides that, from the previous relationship, it was determined that a bigger volume also means a longer flow distance, so the area affected by this disaster will be larger too.

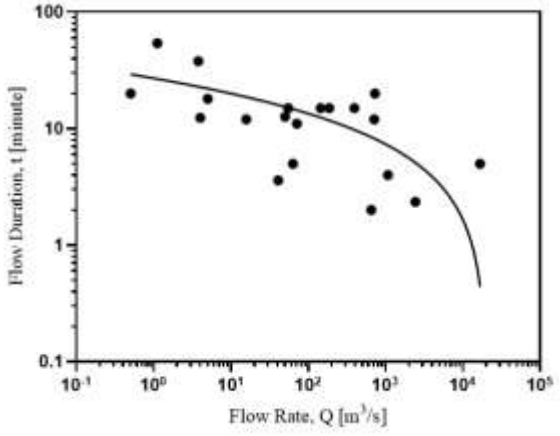

Figure 10. Flow Rate-Flow Duration Relationship

The flow depth and flow duration relationship can be seen in Fig. 11. The trend shows a negative correlation between these parameters, which means as the flow depth gets deeper, the flow duration will be faster. On the other side, when the flow depth decreases, the flow duration increases, so the flow will be slower. The relationship can be represented by Eq. (9).

$$t = 89.15 - \frac{63.32}{h^{-0.134}} \tag{9}$$

This relationship is related to the previous relationship (i.e., flow rate-flow duration). When the flow depth increases, the cross-section of the flow will also increase. A larger cross-section means the flow rate will get bigger. Therefore, the flow duration will decrease along with the flow rate increment.

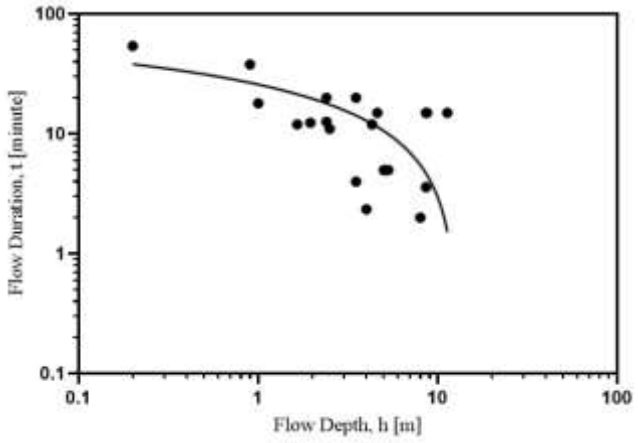

Figure 11. Flow Depth-Flow Duration Relationship

Lastly, Fig. 12 shows the relationship between flow width and flow distance. The trend shows a positive correlation. That means the flow distance will also increase when the flow width increases. On the contrary, a smaller flow width means the flow distance will also decrease. Eq. (10) that was obtained from the trendline represents the relationship between these parameters.

$$L = 160.981\ e^{0.012\ B} \tag{10}$$

This last relationship portrays the mudflow shape, which will always be elongated. It is because as the flow gets wider, the flow length or distance will increase exponentially. Therefore, the length of the mudflow will always be greater than its width.

ISBN: 978-1-63248-195-5 DOI: 10.15224/ 978-1-63248-195-5-13

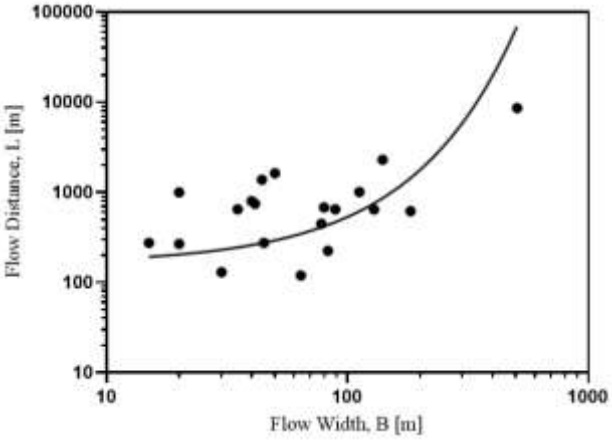

Figure 12. Flow Rate-Flow Duration Relationship

Two case studies from Indonesia and Switzerland are used to validate the empirical models. The way to validate is by comparing the calculated parameters and the parameters obtained from the actual conditions in the field. Jemblung Mudflow is chosen as the representative of the case study from Indonesia. The measured parameters can be seen in Table 1, Table 2, and Table 3. Whereas for the case study from Switzerland, Pont Bouquin mudflow is chosen. Table 4 shows the measured parameters of the Pont Bourquin mudflow.

TABLE IV. PONT BOURQUIN, SWITZERLAND MUDFLOW PARAMETERS [32]

Slope Angle, θ [°]	30
Flow Distance, L [m]	240
Flow Width, B [m}	35
B/L	0.14
Flow Depth, h [m]	10
Flow Duration, t [min]	3
Flow Rate, Q [m^3/s]	2100
Volume, V [m^3]	5000
Flow Velocity, u [m/s]	12
Soil Type	ML
SG	2.75
w	87.40
LL [%]	47.00
PL [%]	14.00
PI {%]	33.00
LI	2.22
Cv	0.29
Yield Stress, τ_y [kPa]	1.30
Viscosity, η [Pa·s]	0.01

The validation for both case studies is done in the table, which can be seen in table 5 for the Jemblung case study and table 6 for the Pont Bourquin case study.

TABLE V. VALIDATION WITH JEMBLUNG MUDFLOW

Parameters	Measured	Calculated	Percentage Error
Flow Distance, L [m]	681.00	481.94[a]	29.23
		513.52[b]	24.59
Viscosity, η [Pa·s]	0.20	0.05	76.14
Yield Stress, τ_y [kPa]	1.46	1.51	3.25
Flow Depth, B [m]	80.00	70.16	12.31
Volume, V [m^3]	56092.52	42237.16	24.70
Flow Duration, t [min]	15.00	11.75[c]	21.67
		11.46[d]	23.58

a. Eq. (3); b. Eq. (10); c. Eq. (8); d. Eq. (9)

From the comparison done in Table 5, it was obtained that seven empirical relationships have a percentage of error below 30%. That means these models are good enough to represent the actual mudflow behaviors. However, the calculated viscosity has a 76.14% error compared to the actual viscosity. It may indicate that the model can only represent the real condition of some mudflow.

TABLE VI. VALIDATION WITH PONT BOURQUIN MUDFLOW

Parameters	Measured	Calculated	Percentage Error
Flow Distance, L [m]	240.00	280.98[a]	17.08
		267.41[b]	11.42
Viscosity, η [Pa·s]	0.01	0.0081	19.30
Yield Stress, τ_y [kPa]	1.30	1.17	9.92
Flow Depth, B [m]	35.00	29.53	15.63
Volume, V [m^3]	5000.00	5663.45	13.27
Flow Duration, t [min]	3.00	5.47[c]	82.28
		2.94[d]	1.89

a. Eq. (3); b. Eq. (10); c. Eq. (8); d. Eq. (9)

Based on the comparison from the Pont Bouquin case study, it can be concluded that seven empirical models have a percentage of error below 20%. It also means that the models can represent the actual mudflow behavior. But the calculated flow duration obtained from Eq. (8) has an 82.28% error compared to the measured flow duration time.

It implies that the model cannot be used to represent all mudflow events.

ISBN: 978-1-63248-195-5 DOI: 10.15224/ 978-1-63248-195-5-13

v. Conclusion

Mudflow is a natural disaster that poses a massive, dangerous threat, but knowledge about this mass movement is limited. This study collects data from twenty case studies, 15 from Indonesia and one from Taiwan, Korea, China, Chile, and Italy. Based on the data, it can be concluded that high plasticity silt is the soil type that is most likely to become mudflow, the obtained C_v values are in the range of 0.29-0.56, and the width-length ratio is in the range of 0.02 – 0.53. Besides that, eight empirical relationships that describe the mudflow behavior are obtained.

The eight relationships are: the flow distance will increase with a steeper slope; as the liquidity index increases, the viscosity will decrease; as the liquidity index increases, the yield stress will decrease; a higher viscosity means the flow gets wider; a larger flow distance means a bigger volume that moved from the source area; as flow rate increases, the flow duration decrease; a deeper flow depth means a smaller flow duration; as flow get wider, the flow length or distance will also increase.

The validation results show that six empirical relationships, Eq. (3), (5), (6), (7), (9), and (10), can accurately represent mudflow behavior because the percentage of error is less than 30%. But the liquidity index-viscosity equation and the flow rate-flow duration equation have a large percentage of error, which means the mudflow events that those equations can represent are limited.

References

[1] U.S. Geological Survey, "Landslide 101," 2018. [Online]. Available: https://www.usgs.gov/programs/landslide-hazards/landslides-101. [Accessed 26 November 2022]

[2] D. M. Cruden and D. J. Varnes, "Landslide types and processes," in *Landslides: investigation and mitigation*, Transportation Research Board Special Report 247, 1996, pp. 36-75.

[3] R. M. Iverson, "The physics of debris flows," *Reviews of Geophysics*, vol. 35, no. 3, pp. 245-296, 1997.

[4] P. Anawe and A. Folayan, Advances in Drilling Fluids Rheology, Lambert Academic Publishing, 2018.

[5] B. Widjaja and S. H.-H. Lee, "Flow box test for viscosity of soil in plastic and viscous liquid states," *Soils and Foundation*, vol. 53, pp. 35-46, 2013.

[6] J. S. O'Brien and P. Y. Julien, "Laboratory analysis of mudflow properties," *Journal of Hydraulic Engineering*, pp. 877-887, 1988.

[7] J. Liu and P. Mason, Essential Image Processing and GIS for Remote Sensing, Wiley-Blackwell, 2009.

[8] D. Petley, "The massive, catastrophic Villa Santa Lucia landslide in Chile: videos and images start to hint at the cause," Advancing Earth and Space Science, 19 December 2017. [Online]. Available: https://blogs.agu.org/landslideblog/2017/12/19/villa-santa-lucia-landslide-2/. [Accessed 26 November 2022].

[9] W. Aila, "Simulasi Mudflow di Sukaresmi Cianjur Menggunakan Program FLO-2D," Universitas Katolik Parahyangan, 2013.

[10] N. Riyanto, "Simulasi pergerakan tanah pada studi kasus longsor di Bantar, Banjarnegara menggunakan program Flo-2D," Universitas Katolik Parahyangan, 2018.

[11] A. Johan, "Pemodelan longsoran pada : studi kasus longsoran Desa Karangrejo dengan Flo-2D dan RAMMS," Universitas Katolik Parahyangan, 2017.

[12] B. Widjaja, "Viscosity determination of soil in plastic and viscous liquid states for elucidating mudflow behavior," National Taiwan University of Science and Technology, 2012.

[13] K. Kamajaya, "Analisis tumbukan longsoran pada pipa PLTP di Kampung Cibitung Desa Margamukti Pangalengan," Universitas Katolik Parahyangan, 2020

[14] D. K. Mulia, "Analisis sensitivitas pengaruh perubahan parameter rheologi pada program FLO-2D dan RAMMS : studi kasus longsor di Desa Banaran, Kecamatan Pulung, Kabupaten Ponorogo, Jawa Timur," Universitas Katolik Parahyangan, 2018.

[15] D. M. WIbowo, "Pengaruh kadar lempung terhadap yield stress dan viskositas : studi kasus gerakan tanah di Desa Pasir Panjang," Universitas Katolik Parahyangan, 2019.

[16] J. S. Prakoso, "Perbandingan hasil analisis pergerakan tanah menggunakan model Bingham dan model Voellmy : studi kasus Desa Songan, Bali," Universitas Katolik Parahyangan, 2017.

[17] J. K. Putra, "Analisis sensitivitas perubahan debit dan durasi longsoran terhadap simulasi mudflow dengan program Flo-2D di Desa Sirnaresmi, Sukabumi," Universitas Katolik Parahyangan, 2019.

[18] M. A. Krisdanto, "Simulasi pengaruh perubahan kadar air terhadap longsoran mudflow menggunakan program Flo-2D : studi kasus Mukapayung - Cililin," Universitas Katolik Parahyangan, 2014.

[19] S. M. B. Naba, "Simulasi terjadinya pergerakan tanah di Dusun Jemblung, Banjarnegara dengan bantuan program FLO-2D," Universitas Katolik Parahyangan, 2015.

[20] D. Pascayulinda, "Kajian teknis studi pergerakan tanah di Jawa dan Bali," Universitas Katolik Parahyangan, 2018.

[21] A. B. Setiawan, "Back analysis for Parungponteng, Tasikmalaya mass movement phenomenon using FLO-2D," Universitas Katolik Parahyangan, 2016.

[22] F. Ulfa, "Debris flow susceptibility analysis based on landslide inventory and run-out modelling in Middle Part of Kodil Watershed, Central Java," Gadjah Mada University, 2017.

[23] G. Samudra, "Morphodynamic Simulation of Kalisari Landslide, Magelang Regency," *Journal of Environment and Geological Hazards*, pp. 82-95, 2018.

[24] H. Baladraf, "Pemodelan pergerakan tanah dan saran tindakan mitigasi pada studi kasus longsoran di Kecamatan Sukajaya Kabupaten Bogor dengan menggunakan Program Flo-2D," Universitas Katolik Parahyangan, 2020.

[25] A. D. Putri, "Perbandingan hasil analisis mudflow menggunakan Program Abaqus dan Flo-2D : studi kasus Umyeonsan Korea Selatan," Universitas Katolik Parahyangan, 2020.

[26] S. Lee, "Analysis of debris flow simulation parameters with entrainment effect: a case study in the Mt. Umyeon," Korea Water Resources Association, vol. 53, no. 9, pp. 637-646, 2020.

[27] M. A. Somos-Valenzuela, "The mudflow disaster at Villa Santa Lucía in Chilean Patagonia: understandings and insights derived from numerical simulation and postevent field surveys," Natural hazards and Earth System Sciences, pp. 2319-2333, 2020.

[28] F. Zhang, "A study of a flow slide with significant entrainment in loess areas in China," *Earth Surface Processes and Landforms*, 2017.

[29] J. Peng, "Heavy rainfall triggered loess–mudstone landslide and subsequent debris flow in Tianshui, China," *Engineering Geology*, 2014.

[30] T. W. J. v. Asch, "Unravelling the multiphase run-out conditions of a slide-flow mass movement," Geomorphology, vol. 230, pp. 161-170, 2015.

[31] M. Berti, "Field observations of a debris flow event in the Dolomites," *Geomorphology*, vol. 29, pp. 265-274, 1999.

[32] S. R. Carriere, "Rheological properties of clayey soils originating from flow-like landslides," Landslides, pp. 1615-1630, 2018.

ISBN: 978-1-63248-195-5 DOI: 10.15224/ 978-1-63248-195-5-13

About Authors:

Budijanto Widjaja, Ph.D., has taught soil mechanics and geotechnical engineering at Parahyangan Catholic University, Indonesia. Nowadays, he is a director of a Center for Geotechnical-hazards (C4GH) and head of geotechnical laboratory. His research interest is the behavior of mudflow, landslides, clay shales, and numerical methods in geotechnical engineering.

Livia Florencia is a third-year student in the Department of Civil Engineering at Parahyangan Catholic University. She has a great interest in geotechnical engineering and water resources management.